Available online at www.sciencedirect.com

ScienceDirect

Mendeleev Commun., 2019, **29**, 215–217

Mendeleev Communications

Photocatalytic properties of SnO_2–SnO nanocomposite prepared *via* pulse alternating current synthesis

Anna A. Ulyankina,*[a] Alexandra B. Kuriganova[a] and Nina V. Smirnova[a,b]

[a] *Platov South-Russian State Polytechnic University (NPI), 346400 Novocherkassk, Russian Federation. E-mail: anya-barbashova@yandex.ru*

[b] *National University of Science and Technology 'MISIS', 119049 Moscow, Russian Federation*

DOI: 10.1016/j.mencom.2019.03.034

A SnO_2–SnO nanocomposite was electrochemically synthesized using pulse alternating current and characterized by XRD, SEM, TEM, UV-VIS DRS, and low-temperature N_2 adsorption/desorption (BET) methods. The photocatalytic activity of nanocomposite was estimated for the degradation of methylene blue dye. The pseudo-first-order reaction constant rate k was calculated to be 79.1×10^{-3} min^{-1}.

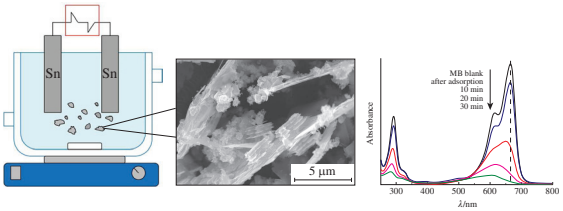

Nowadays, harmful water contaminants, which are difficult to degrade by conventional physical and chemical methods, become a major issue as the source of environmental pollution. Thereby, a wastewater treatment requires inexpensive and suitable technologies. One among the best and green strategies for the purification of water resources from organic contaminants is heterogeneous photocatalysis. Different semiconductor materials (TiO_2, ZnO, SnO_2, CdS, *etc*.) have been investigated for environmental applications.[1–4] Among various nanomaterials, tin oxide has attracted a great interest of researchers due to its outstanding physical and chemical properties. Tin oxide usually exists in two phases (SnO_2 and SnO). The SnO_2 nanoparticles have already been utilized for the water treatment.[5,6] However, SnO as a photocatalyst has not been intensively evaluated in comparison with SnO_2. Reports on preparation of SnO_2–SnO materials are scarce. However, several works revealed that coupled catalytic systems such as SnO_2–SnO nanocomposite can enhance the rate of photocatalytic dye degradation as compared to the pure SnO_2 nanoparticles due to the inhibition of electron–hole recombination process.[7,8] It is well known that the photocatalytic properties of materials depend on their morphology and particle size. Thus, various methods such as hydrothermal,[9] chemical co-precipitation,[10] and sol–gel[11] were developed for the preparation of SnO_2–SnO nanocomposites possessing different structures. However, the majority of these approaches require toxic chemicals, critical reaction conditions as well as harsh and complicated procedures. Therefore, the development of an efficient method to obtain SnO_2–SnO nanocomposite with high photocatalytic activity without any templates under mild conditions remains a crucial problem.

This work was aimed at the development of new electrochemical approach to concurrent green synthesis of SnO_2–SnO nanocomposite based on the oxidation of Sn electrodes, wherein the pulse alternating current (PAC) acts as a clean oxidant.† The synthesis of other metal oxide-based materials such as CuO_x, ZnO, and Pt/TiO_2 nanocomposites using PAC has already been described in our previous reports.[12–14]

Phase composition of the as-prepared SnO_2–SnO nanocomposite was examined by the powder X-ray diffraction (XRD) analysis (Figure 1).‡ As one can see, the X-ray diffractogram contains two sets of well resolved Bragg reflections, which correlate perfectly to the indexed tetragonal SnO_2 and tetragonal SnO phases. Moreover, the absence of any other diffraction peaks indicates the high purity of synthesized SnO_2–SnO nanocomposite.

Previously, we demonstrated the possibility of preparing pure SnO_2 nanoparticles for lithium-ion batteries under PAC treatment using 2 M NaCl as the electrolyte.[15] However, such SnO_2 nanoparticles possessing the size of 11–16 nm and specific surface area of 82.5 m^2 g^{-1} exhibited a very high adsorption ability but the poor photocatalytic activity. It can be attributed to the blocking of photocatalyst active sites during the adsorption.[16]

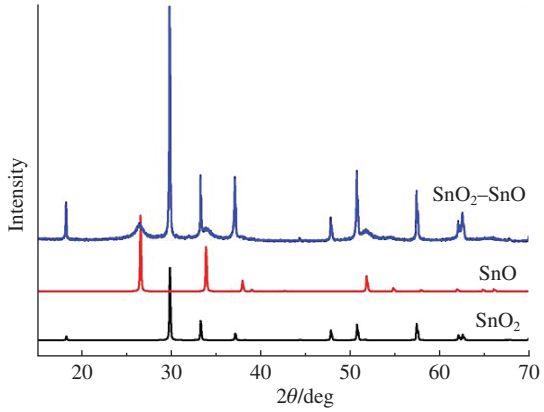

Figure 1 XRD pattern of the prepared SnO_2–SnO nanocomposite and standard ICDD patterns for SnO_2 and SnO.

† Two tin electrodes were placed in 1 M aqueous NaF solution and connected to a PAC source.[12–14] The average current density was 1.0 A cm^{-2}. The tin electrodes were oxidized upon PAC treatment for 1 h to give SnO_2–SnO nanocomposite. The precipitate was isolated by filtration, washed with deionized water, and dried at 80 °C.

‡ The XRD analysis was performed on a Bruker D2 Phaser instrument using CuKα radiation (λ = 1.5406 Å) with a step size of 0.02° (2θ).

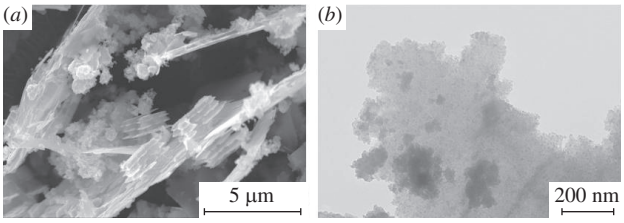

Figure 2 (*a*) SEM and (*b*) TEM images of SnO_2–SnO composite prepared by PAC synthesis.

The surface morphology of prepared sample was revealed by SEM and TEM (Figure 2).§ The images clearly confirmed the formation of small aggregated nanoparticles on the surface of large plates.

It is commonly believed that the photocatalytic activity is mainly related to the amount of active sites on the catalyst surface. The Brunauer–Emmett–Teller (BET) surface area of SnO_2–SnO nanocomposite was calculated to be 35.0 m^2 g^{-1}.¶

Figure 3 shows the UV-VIS diffuse reflectance (UV-VIS DRS) spectrum†† of SnO_2–SnO nanocomposite recorded in the percentage reflectance mode in the range from 200 to 800 nm. The direct band gap (see inset in Figure 3) was calculated to be 3.3 eV. The resulting band gap value is consistent with that (3.31 eV) reported for a SnO_2–SnO heterostructure prepared by hydrothermal method followed by the post-annealing.[17]

The formation of tin oxides in alkaline solutions (pH of 1 M NaF is about 9) is a complex process comprising several steps:[15,18]

$$Sn + 2OH^- \leftrightarrow Sn(OH)_2 + 2e^- \quad (1)$$

$$Sn(OH)_2 + 2OH^- \leftrightarrow Sn(OH)_4 + 4e^- \quad (2)$$

$$Sn(OH)_4 \leftrightarrow SnO_2 + 2H_2O \quad (3)$$

$$Sn(OH)_2 \leftrightarrow SnO + H_2O \quad (4)$$

To evaluate the photocatalytic performance of the SnO_2–SnO nanocomposite, the degradation of methylene blue (MB) dye under UVA irradiation was carried out.‡‡ Figure 4(*a*) shows changes in the absorption spectrum of MB during its photodegradation in the presence of SnO_2–SnO nanocomposite. One can see that the intensity of bands at 664 and 612 nm decreases

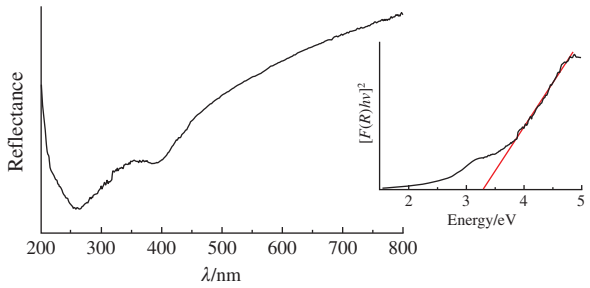

Figure 3 The UV-VIS DRS spectrum and direct band gap (inset) of SnO_2–SnO nanocomposite.

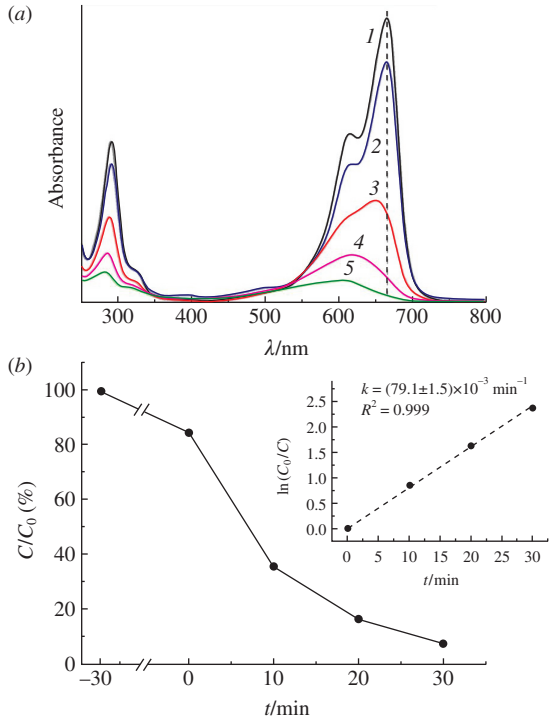

Figure 4 (*a*) Time-dependent UV-VIS absorption spectra: (*1*) MB blank, (*2*) after adsorption and after irradiation within (*3*) 10, (*4*) 20 and (*5*) 30 min; (*b*) C/C_0 *vs*. irradiation time plot, inset shows pseudo-first order kinetics plot of MB degradation in the presence of SnO_2–SnO nanocomposite upon UVA irradiation.

rapidly with increasing irradiation time, which indicates the photodegradation of MB dye. The color of MB solution was also gradually lightened. This result suggests that the sulfur–nitrogen conjugated system was destroyed.[19] Moreover, the blue shift of two bands was observed upon prolonged irradiation probably due to the demethylation of MB molecules and their conversion into other intermediates.[19]

The degree of photodegradation (C/C_0) as a function of time was calculated with respect to the maximum absorbance of MB dye [Figure 4(*b*)]. The values C_0 and C are the initial concentration of dye and its concentration at the reaction time t, respectively. The photocatalytic degradation efficiency was found to be 92.1% within 30 min. This result suggests that the as-prepared SnO_2–SnO nanocomposite possesses an excellent photocatalytic activity.

The MB decomposition under UVA irradiation was well fitted to a pseudo-first-order kinetic model. The plot of $\ln(C_0/C)$ *vs*. irradiation time [see Figure 4(*b*), inset] allowed us to estimate the pseudo-first-order rate constant k (k = 0.0791 min^{-1}) by taking the slope of linear plot. The curve exhibits a good linear correlation, and the value of correlation coefficient (R^2) is extremely close to 1.

The comparison between photocatalytic activities of tin oxides towards the MB degradation under UVA light is given in Table 1. The enhanced photocatalytic activity of our nanocomposite may be attributed to an inhibition of photogenerated electron-hole recombination process by the efficient charge separation due to the formation of coupled semiconductor system of SnO_2–SnO.

§ TEM images were acquired in a bright-field TEM mode at 100 kV accelerating voltage using a Hitachi HT7700 transmission electron microscope. SEM images were obtained using a PHILIPS XL30 scanning electron microscope.

¶ BET measurements were performed on a Quantachrome NOVA 1200e instrument at 77.3 K. The specific surface area was determined according to the BET method.

†† UV-VIS DRS spectra were recorded on a Shimadzu UV-2600 spectrophotometer using $BaSO_4$ as the background and transformed according to the Kubelka–Munk function [$F(R) = (1 - R)^2/2R$, wherein R is the absolute reflectance of sample and $F(R)$ is proportional to the extinction coefficient α].

‡‡ A Hamamatsu LC8 Mercury-Xenon UV-VIS combined lamp (Hamamatsu Photonics, Shizuoka) with the main irradiation wavelength of 365 nm was used as the light source. The experiments were performed with MB solution (10 ppm, 50 ml) containing the catalyst (50 mg). Prior to UV irradiation, the solution was ultrasonically treated and then stirred for 30 min in darkness in order to reach the adsorption–desorption equilibrium of the dye on the photocatalyst surface. The dye solution was exposed to UV irradiation under constant stirring. The aliquots (2 ml) were sampled after time intervals of 10 min and analyzed for variations in the absorbance at 664 nm of MB dye using a Shimadzu UV-1800 UV-VIS spectrophotometer.

Table 1 Comparison between photocatalytic activities of various tin oxides towards the MB degradation.

Type of catalyst	Synthetic method	Catalyst loading/ g dm^{-3}	MB concentration/ mg dm^{-3}	Light source	t/min	Rate constant k/10^{-3} min^{-1}	Reference
SnO_2 nanotubes	Template-based liquid phase deposition	0.1	10	four 100 W Xe lamps (λ = 365 nm)	180	13.6	20
SnO_2 nanoparticles	Sol-gel method	1	6.4	high pressure Hg lamp (λ = 254 nm, lamp power was not specified)	120	6.3	21
SnO_2 nanocrystals	Direct precipitation method	1	40	125 W low-pressure Hg lamp (λ = 254 nm)	120	25.8	22
SnO nanosheets	Dissolution–precipitation	1	10	15 W Hg lamp (λ was not specified)	600	10.7	23
SnO_2–SnO nanocomposite	Semisolvothermal synthesis	0.5	10	400 W Hg vapor lamp (λ was not specified)	180	6.2	8
SnO_2–SnO nanocomposite	PAC synthesis	1	10	200 W Hg–Xe lamp (λ = 365 nm)	30	79.1	This work

In conclusion, we have successfully prepared the SnO_2–SnO nanocomposite *via* new electrochemical synthesis under the pulse alternating current conditions using 1 M aqueous NaF solution as the electrolyte, which was confirmed by the XRD pattern. The prepared nanocomposite exhibits the high photocatalytic activity towards the MB degradation under UVA irradiation. The calculated pseudo-first-order rate constant of 0.0791 min^{-1} is higher by a factor of 5–10 than those of various tin oxide-based photocatalysts reported to date. Therefore, the developed synthesis may be a promising way to obtain SnO_2–SnO nanocomposites for the removal of organic pollutants in wastewater and other applications.

This work was supported by the Russian Science Foundation (grant no. 14-23-00078). The authors are also grateful to the Shared Research Center 'Nanotechnologies' at the Platov South-Russian State Polytechnic University (NPI).

References

1 C. Byrne, G. Subramanian and S. C. Pillai, *J. Environ. Chem. Eng*., 2018, **6**, 3531.
2 S. Yu. Kochev, Yu. N. Bubnov, S. S. Abramchuk, O. Yu. Antonova, P. M. Valetsky and Yu. A. Kabachii, *Mendeleev Commun*., 2017, **27**, 310.
3 I. A. Kovalev, A. A. Petrov, O. A. Ibragimova, A. V. Shokod'ko, A. S. Chernyavskii, E. A. Goodilin, K. A. Solntsev and A. B. Tarasov, *Mendeleev Commun*., 2018, **28**, 541.
4 O. I. Gyrdasova, M. A. Melkozerova, I. V. Baklanova, L. Yu. Buldakova, N. S. Sycheva, V. N. Krasil'nikov and M. Yu. Yanchenko, *Mendeleev Commun*., 2017, **27**, 410.
5 A. Bhattacharjee, M. Ahmaruzzaman, T. B. Devi and J. Nath, *J. Photochem. Photobiol. A*, 2016, **325**, 116.
6 E. Abdelkader, L. Nadjia, B. Naceur and B. Noureddine, *J. Alloys Compd*., 2016, **679**, 408.
7 K. Santhi, C. Rani and S. Karuppuchamy, *J. Alloys Compd*., 2016, **662**, 102.
8 A. Roy, S. Arbuj, Y. Waghadkar, M. Shinde, G. Umarji, S. Rane, K. Patil, S. Gosavi and R. Chauhan, *J. Solid State Electrochem*., 2017, **21**, 9.
9 Y.-C. Chang, J.-C. Lin, S.-Y. Chen, L.-Y. Hung, Y.-R. Lin and C.-Y. Chen, *Mater. Res. Bull*., 2018, **100**, 429.
10 N. C. Horti, M. D. Kamatagi, N. R. Patil, M. N. Wari and S. R. Inamdar, *Optik*, 2018, **169**, 314.
11 S. Bagherian and A. K. Zak, *Mater. Sci. Semicond. Process*., 2016, **56**, 52.
12 A. Ulyankina, I. Leontyev, M. Avramenko, D. Zhigunov and N. Smirnova, *Mater. Sci. Semicond. Process*., 2018, **76**, 7.
13 A. Ulyankina, I. Leontyev, O. Maslova, M. Allix, A. Rakhmatullin, N. Nevzorova, R. Valeev, G. Yalovega and N. Smirnova, *Mater. Sci. Semicond. Process*., 2018, **73**, 111.
14 A. B. Kuriganova, I. N. Leontyev, A. S. Alexandrin, O. A. Maslova, A. I. Rakhmatullin and N. V. Smirnova, *Mendeleev Commun.*, 2017, **27**, 67.
15 A. B. Kuriganova, C. A. Vlaic, S. Ivanov, D. V. Leontyeva, A. Bund and N. V. Smirnova, *J. Appl. Electrochem*., 2016, **46**, 527.
16 B. Soman, S. Challagulla, S. Payra, S. Dinda and S. Roy, *Res. Chem. Intermed*., 2018, **44**, 2261.
17 H. Yu, T. Yang, Z. Wang, Z. Li, Q. Zhao and M. Zhang, *Sens. Actuators, B*, 2018, **258**, 517.
18 F. I. Pires, E. Joanni, R. Savu, M. A. Zaghete, E. Longo and J. A. Varela, *Mater. Lett*., 2008, **62**, 239.
19 J. Lin, Z. Luo, J. Liu and P. Li, *Mater. Sci. Semicond. Process*., 2018, **87**, 24.
20 A. Sadeghzadeh-Attar, *Sol. Energy Mater. Sol. Cells*, 2018, **183**, 16.
21 M. A. Ahmed, M. F. A. Messih, E. F. El-Sherbeny, S. F. El-Hafez and A. M. M. Khalifa, *J. Photochem. Photobiol., A*, 2017, **346**, 77.
22 X. Wan, R. Ma, S. Tie and S. Lan, *Mater. Sci. Semicond. Process*., 2014, **27**, 748.
23 W. Liu, L. Yin, R. Zhang, H. Yang, J. Ma and W. Cao, *Nanotechnology*, 2018, **29**, 284002.

Received: 13th August 2018; Com. 18/5668